Journal of Alloys and Compounds 503 (2010) 370–374

Contents lists available at ScienceDirect

Journal of Alloys and Compounds

journal homepage: www.elsevier.com/locate/jallcom

Optimization of carbon coatings on $LiFePO_4$: Carbonization temperature and carbon content

Xiaoke Zhi, Guangchuan Liang*, Li Wang, Xiuqin Ou, Limin Gao, Xiaofei Jie

Institute of Power Source & Ecomaterials Science, Hebei University of Technology, Tianjin 300130, China

ARTICLE INFO

Article history:
Received 12 November 2009
Received in revised form 22 February 2010
Accepted 25 February 2010
Available online 3 March 2010

Keywords:
$LiFePO_4$
Carbon coating
Carbonization temperature
Carbon content
Electrochemical performance

ABSTRACT

$LiFePO_4$/C composite cathode materials were synthesized by carbothermal reduction route using inexpensive $FePO_4$ as raw material and glucose as reductive agent and carbon source. The samples were characterized by X-ray diffraction (XRD), scanning electron microscope (SEM), transmission electron microscope (TEM), Fourier transform infrared (FTIR), laser Raman spectroscopy and constant-current charge/discharge test. The results indicate that the structure of conductive carbon, depending on the carbonization (synthesis) temperature, is closely related to the electrochemical performance of $LiFePO_4$/C composites. The quality of carbon coating on the $LiFePO_4$ particle surface is determined by the carbon content, and only a proper carbon content (about 3%) can lead to a more uniform carbon distribution. Electrochemical results show that the optimal sample synthesized at 700 °C and with a carbon content of 3.1%, delivers a high discharge capacity of 116.0 mAh g^{-1} at 5*C* rate, and the discharge capacity shows little degradation after 100 cycles at 2*C* rate. The excellent high-rate dischargeability and cycling performance of the optimal sample can be attributed to its high carbonization degree and uniform carbon coating.

1. Introduction

$LiFePO_4$ has been considered to be the preferred cathode material for electric vehicle battery due to its good features, such as abundance in raw materials, environmental friendliness, perfect cycling performance, safety and so on [1–5]. However, the high-rate dischargeability and low temperature performance of $LiFePO_4$ cathode materials are restricted by its relatively poor electronic conductivity and low Li^+ diffusion rate [6]. Currently, some researchers suggested that the synthesis of fine materials (nano-sized materials) completely coated with conductive carbon was an effective means of eliminating these problems [7,8]. The carbon coating could be implemented generally through adding organic compounds or polymers in precursor during synthesis process. However, the thermal decomposition of those organic compounds is a very complex process, including covalent bond fracturing and forming, carbon chain reconstructing and so on, and the structure and properties of conductive carbon will be ultimately determined by these reactions. Many researches have indicated that the carbonization temperature is a key factor affecting pyrolytic carbon structures [9,10]. However, people tend to focus on the effect of synthesis temperature on particle size and crystallinity in the synthesis process of $LiFePO_4$, the influence of conductive carbon structure on material performances is rarely studied. On the other hand, just a spot of carbon addition could greatly reduce the tap density of $LiFePO_4$ materials [11], leading to the decrease of energy density. So the carbon coating should be optimized in order to achieve the improvement in electrochemical performance of $LiFePO_4$/C composites.

2. Experimental

Stoichiometric amounts of nano-sized $FePO_4$ (A.R, Liangnuo, Tianjin), Li_2CO_3 (A.R, Zhongli, Sichuan) and glucose were mixed and then ground uniformly in a mortar. The mixture was transferred to a tube furnace and fired at different temperatures for 12 h under flowing nitrogen to synthesize $LiFePO_4$/C composites.

The morphology and microstructure of the prepared sample powders were observed using scanning electron microscopy (SEM) with a FEI SIRION microscope and transmission electron microscopy (TEM) with Philips Tecnai F20. The crystal structures were analyzed by X-ray diffraction (XRD) on a Rigaku-D/MAX-2550PC diffractometer with Cu Kα radiation. The structure of carbon was analyzed using an inVia micro laser Raman spectroscopy. The Fourier transform infrared (FTIR) absorption spectra of all samples were recorded in 500–2500 cm^{-1} range at room temperature using a VERTEX 80V FTIR spectrometer. The electronic conductivity of the samples was measured using two-point probe method.

The electrochemical measurement was made with the CR2430 pattern. The cathode electrode was made in the following way. The $LiFePO_4$/C powder was mixed with acetylene black and polytetrafluoroethylene (PTFE) in a weight ratio of 80:15:5, then rolled into a 0.16 mm thick sheet and cut into pellets. With the lithium metal anode as anode, a Celgard 2400 microporous membrane as separator, and 1 mol L^{-1} $LiPF_6$ in ethylene carbonate (EC)–dimethyl carbonate (DMC, 1:1 in volume) as electrolyte, the cell was assembled in a nitrogen-filled (RH < 3%) glove box. The charge/discharge test was performed between 2.3 and 4.2 V (vs. Li/Li^+) with LAND battery testing

---

* Corresponding author. Tel.: +86 022 60204308; fax: +86 022 26564850.
E-mail addresses: liangguangchuan@hebut.edu.cn, zxkb440@163.com (G. Liang).

0925-8388/$ – see front matter © 2010 Elsevier B.V. All rights reserved.
doi:10.1016/j.jallcom.2010.02.173

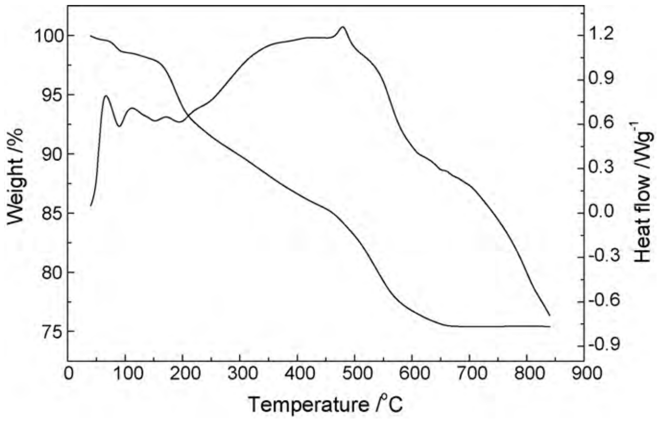

Fig. 1. TG/DSC curves of the precursor from room temperature to 850 °C with a heating rate of 10 °C/min.

system. The electrochemical impedance spectra of all samples were measured in the range of 1 to 1 × 10^6 Hz using a CHI660C electrochemical workstation.

3. Results and discussion

Fig. 1 shows the TG/DSC curves of the precursor from room temperature to 850 °C with a heating rate of 10 °C min^{-1} in a nitrogen flow rate of 100 mL min^{-1}. From Fig. 1, we can see that the TG curve shows three obvious weight loss steps over the temperature range from ambient to 600 °C. The peak at around 90 °C in DSC curve can be assigned to the loss of absorption water of the mixture. The weight loss from 150 to 250 °C in TG curve is related to the thermal decomposition of glucose. And the exothermic peak at 480 °C in DSC curve accompanied by a weight loss in TG curve maybe ascribed to the carbothermal reduction and the formation of $LiFePO_4$, which indicates that the synthesis temperature must be higher than 480 °C. Therefore, we choose four different synthesis temperatures of 600, 650, 700 and 800 °C to obtain $LiFePO_4$/C composites with high crystallinity.

Fig. 2 shows the XRD patterns of $LiFePO_4$/C composites synthesized at 600, 650, 700 and 800 °C, respectively. The main phase of all samples can be identified as $LiFePO_4$ with an ordered olivine structure indexed to orthorhombic Pnma (JCPDS card number: 83-2092). No impurities are detected in the XRD patterns. On the other hand, the narrow diffraction peaks and high diffraction intensity indicate that all samples have high crystallinity.

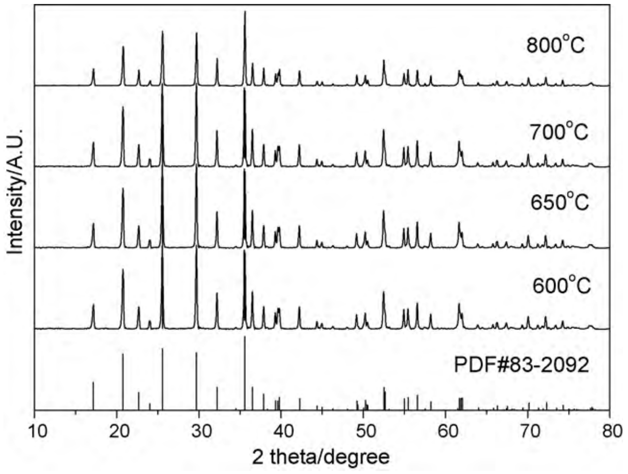

Fig. 2. XRD patterns of $LiFePO_4$/C composites synthesized at different temperatures.

Table 1
The electronic conductivity (σ) and carbon content of $LiFePO_4$/C composites synthesized at different temperatures.

Synthesize temperatures (°C)	Carbon content (%)	σ (S/cm)
600	3.37	3.75×10^{-4}
650	3.10	2.55×10^{-3}
700	2.98	8.71×10^{-2}
800	2.91	1.19×10^{-1}

Table 1 lists the carbon content and electronic conductivity of $LiFePO_4$/C composites synthesized at different temperatures. From Table 1, we can see that with similar carbon content of about 3%, the electronic conductivity of samples increases with the synthesis temperature increasing, indicating that the synthesis or carbonization temperature shows an obvious influence on the electronic conductivity of $LiFePO_4$/C composites. Fig. 3 shows the FTIR curves of carbonized products of glucose at 600, 650, 700 and 800 °C, respectively. The peaks at 740–870 cm^{-1} could be ascribed to C–H bond bending vibration, and the peaks at 1030–1110 cm^{-1} could be ascribed to –C–O–C bond stretching vibration, indicating that the carbon materials carbonized at 600 and 650 °C still contain large amounts of C–H bonds and oxygen-containing groups. When the carbonization temperature increases to 700 and 800 °C, the C–H bonds gradually disappear and the main absorption peaks could be ascribed to C–C bond vibration. The peaks at 1523.7 and 1423.4 cm^{-1} could be ascribed to –C=C– ring stretching vibration of microcrystalline graphite, indicating that carbonization degree of the conductive carbon increases with the synthesis temperature increasing.

The carbon structure is closely related to the carbonization degree. In order to study the conductive carbon structure of $LiFePO_4$/C composites, the Raman spectra test was carried out, and the results are shown in Fig. 4. All Raman spectra consist of a relatively small band at 940 cm^{-1}, which corresponds to the symmetric PO_4 stretching vibration in $LiFePO_4$, and intense broad bands at 1350 and 1590 cm^{-1}, which can be ascribed to the characteristic Raman spectra of carbon film. The bands at 1590 cm^{-1} mainly corresponds to graphitized structured carbon of G band, while that at 1350 cm^{-1} corresponds to disordered structured carbon of D band [12,13]. The graphitized carbon contains sp^2 hybrid bonding, which is positively correlated with the electronic conductivity of carbon, and the disordered carbon mainly corresponds to sp^3 hybrid bonding. In fact, the Raman spectra contain several overlapping absorption bands in range of 1000–1700 cm^{-1} [13–15]. In

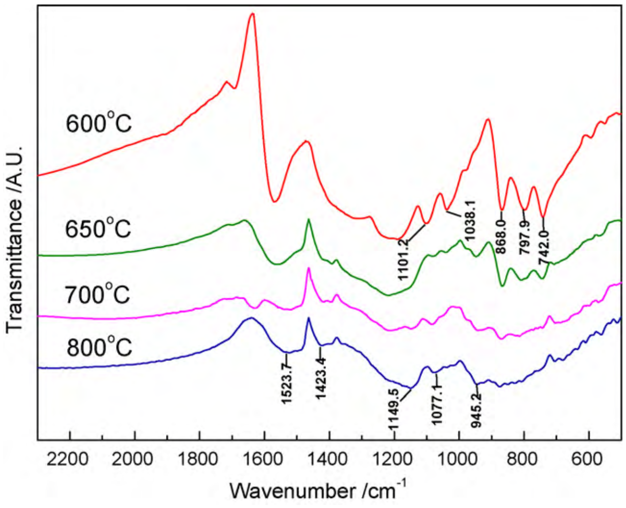

Fig. 3. FTIR curves of carbonized products of glucose at different temperatures.

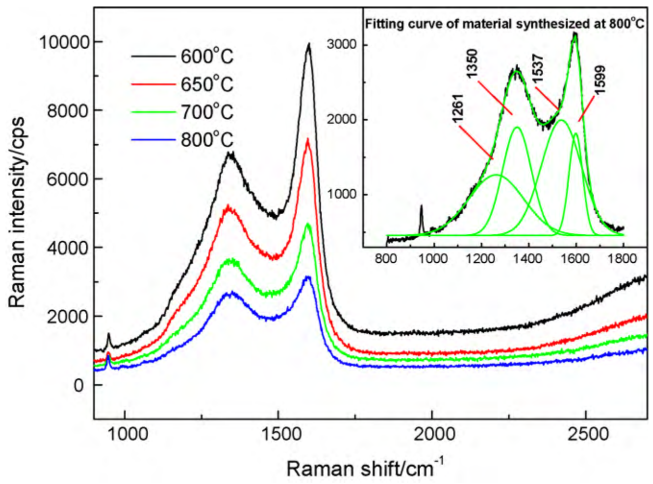

Fig. 4. Raman shift of $LiFePO_4$/C composites synthesized at different temperatures, the internal picture is the fitting curve of material synthesized at 800 °C.

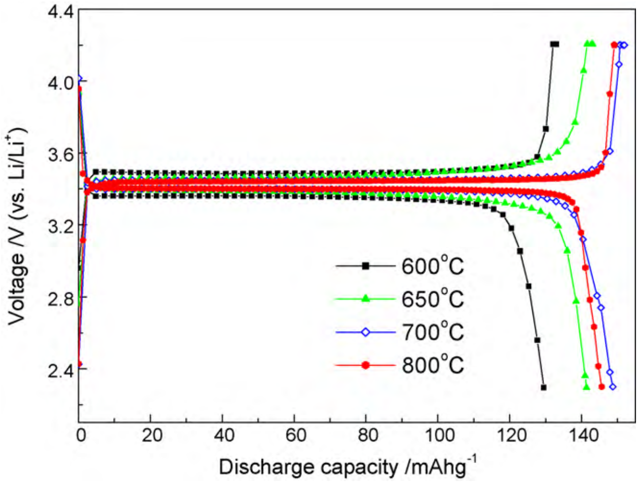

Fig. 5. Initial charge/discharge curves of $LiFePO_4$/C composites synthesized at different temperatures at 0.2*C* rate.

order to analyze the results better, the Raman spectra were processed by four Gaussian bands fitting. Those four fitting bands are located at 1261, 1350, 1537 and 1599 cm^{-1}, respectively, and the band positions vary very little between samples. The bands at 1350 and 1599 cm^{-1} can be assigned to sp^2-type structure, and the others to sp^3-type. The integrated intensity ratios of sp^3/sp^2 of $LiFePO_4$/C composites synthesized at different temperatures are 2.57, 2.21, 1.95 and 1.67, respectively, which indicates that the graphitization degree increases as the carbonization temperature increases, thus leading to the enhancement of electronic conductivity of $LiFePO_4$/C composite materials.

Fig. 5 shows the initial charge/discharge curves of $LiFePO_4$/C composites synthesized at different temperatures at 0.2*C* rate. From Fig. 5 it can be seen that the initial discharge capacity of materials increases gradually as the synthesis temperature and electronic conductivity increase. The initial discharge capacity of the sample synthesized at 600 °C is only 130.0 mAh g^{-1}. And the material synthesized at 700 °C shows a higher discharge capacity of about 148.7 mAh g^{-1}, indicating that the discharge capacity of materials is directly correlated with the increased amounts of sp^2-type carbon and the decreased levels of disordered carbon. The charge and discharge potential difference of the sample synthesized at 600 °C is about 150 mV, while that of the sample synthesized at 700 °C is only about 35 mV, indicating that the polarization of materials is slightly suppressed with synthesis temperature increasing, which could be attributed to the improvement of electronic conductivity of materials. But the sample synthesized at 800 °C has a decreased discharge capacity of about 145 mAh g^{-1}, which maybe due to its excessive particle growth. From the above discussion, it can be concluded that the optimal synthesis temperature is 700 °C.

The conductive carbon has two effects on $LiFePO_4$/C composites during synthesis process, that is, improving electronic conductivity of materials and preventing particle growth. According to Wang's research [8], the particle size and electrochemical polarization can

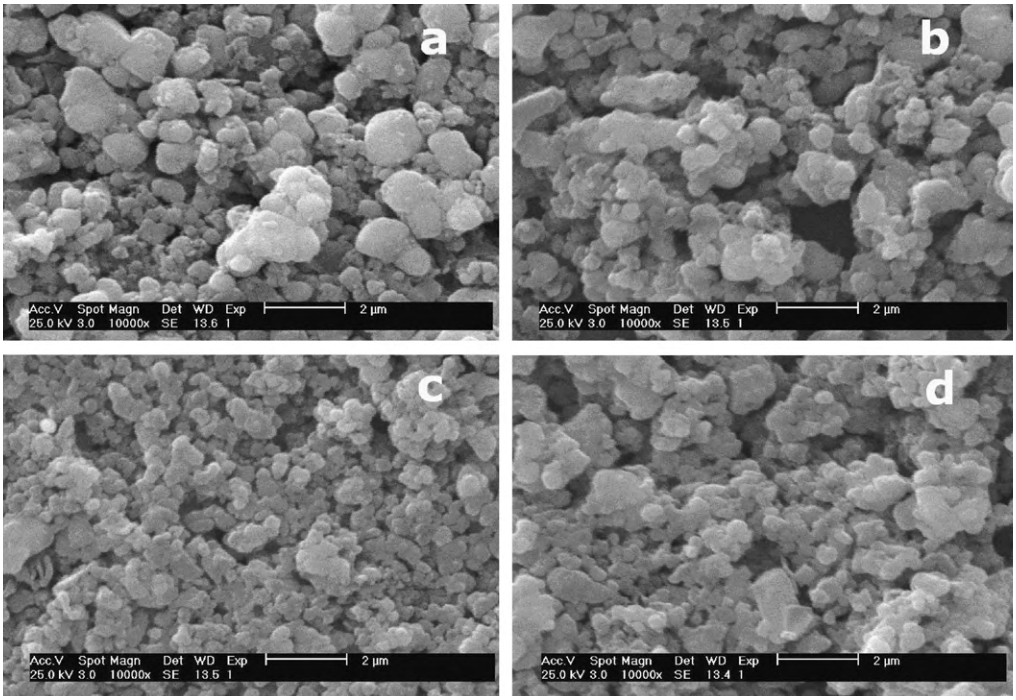

Fig. 6. SEM images of $LiFePO_4$/C composites with various amounts of residual carbon: (a) LFP1, (b) LFP2, (c) LFP3, (d) LFP4.

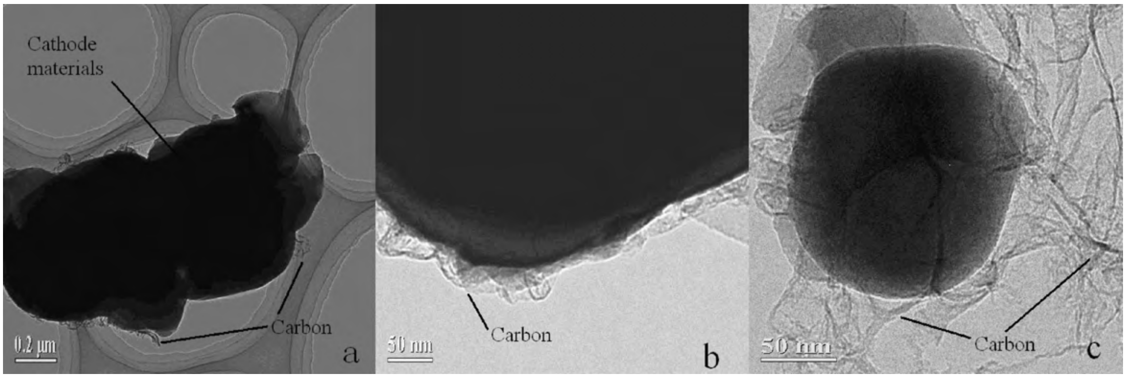

Fig. 7. TEM images of $LiFePO_4/C$ composites with various amounts of residual carbon: (a) LFP1, (b) LFP3, (c) LFP4.

be reduced effectively only when $LiFePO_4$ particle surface is coated uniformly by conductive carbon, but the carbon coating status is correlated with the carbon content. On the other hand, just a small amount of carbon addition could greatly reduce the tap density of $LiFePO_4$ materials. According to the above discussions, it is essential to optimize the carbon content in the materials in order to achieve high power without an undue sacrifice of energy density.

Four $LiFePO_4/C$ composite materials, with carbon contents of 0.9, 2, 3.1 and 5%, respectively, are synthesized at 700 °C, which are denoted as LFP1, LFP2, LFP3 and LFP4, respectively. A series of SEM micrographs (Fig. 6) reveal the morphology change of the samples. As shown in Fig. 6, with the increase of carbon content, a significant decrease in particle size and a more uniform particle size distribution are observed. However, the particle size of sample LFP4 increases abnormally, which maybe caused by the agglomeration of the excessive carbon.

In order to study the effect of carbon content on the carbon coating status, TEM observations were carried out and the results are shown in Fig. 7. It is clear that the samples show different carbon distributions on $LiFePO_4$ particle surface. Sample LFP1 only contains 0.9% carbon, which is not enough to spread throughout the substrate particles, thus leading to the nonuniform carbon coating, as shown in Fig. 7(a). When the carbon content is about 3.1% (LFP3), the carbon coating is comparatively more uniform, and the conductive carbon spreads all over the particles, which is believed to be the optimal carbon distribution status to inhibit particle growth. As for sample LFP4, although the active materials are also coated completely by carbon, the carbon agglomerates formed by excessive carbon around particles cannot effectively inhibit the particle growth but lead to larger particle size. It can be concluded that the carbon content maybe a critical factor for the carbon distribution around particles, and the surfaces cannot be coated effectively until the carbon content reaches a critical value (about 3%). Therefore, proper carbon content always leads to a more uniform carbon distribution and, consequently, a more homogeneous and small particle size of active materials.

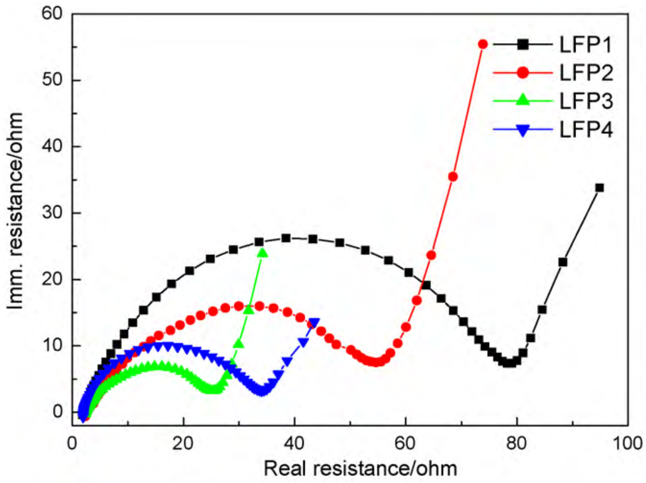

Fig. 8. The impedance spectra of the samples with different carbon contents.

Fig. 8 shows the impedance spectra of the samples with different carbon contents. The impedance spectra are combinations of a depressed semicircle in high-frequency region and a straight line in low-frequency region. The high-frequency semicircle is related to the charge transfer resistance, while the spike at the low frequency end indicates the Warburg impedance of long-range Li-ion diffusion [16–18]. As shown in Fig. 8, the charge transfer resistance of sample LFP1, LFP2, LFP3 and LFP4 are about 80, 58, 25 and 37 Ω, respectively. It is believed that the decrease of charge transfer resistance is beneficial to the kinetic behaviors during charge/discharge process, thus leading to the improvement of electrochemical performance of materials. On the other hand, the impedance spectra also indicate that, when the carbon contents are appropriate, the Li-ion can freely pass the carbon layer, which maybe due to the porous structure of carbon, but the excessive carbon may suppress the Li-ion diffusion in the carbon layer.

Fig. 9 shows the cycling performance curves of the carbon-coated $LiFePO_4$ at various charge–discharge rates. As shown in Fig. 9, the initial discharge capacities of samples LFP1, LFP2, LFP3 and LFP4 at 0.2*C* rate are 150.0, 149.1, 147.5 and 145.6 mAh g^{-1},

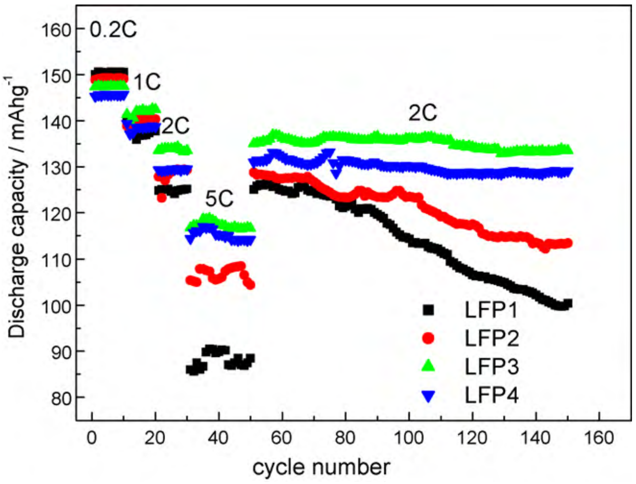

Fig. 9. The cycling performance curves of the samples with different carbon contents at various discharge rates.

Table 2
The electronic conductivity (σ) of $LiFePO_4$/C composites with different carbon contentions.

Samples	σ (S/cm)
LFP1	5.45×10^{-3}
LFP2	9.25×10^{-3}
LFP3	7.61×10^{-2}
LFP4	1.07×10^{-1}

respectively. It is clear that the discharge capacity is decreased with the increase of carbon contents, which maybe due to the remarkable increase of electronic conductivity and the inactive carbon. As shown in Table 2, compared with pure $LiFePO_4$, the carbon-coated $LiFePO_4$ composites exhibit a $\sim 10^6$ to 10^8 increase in electronic conductivity, thus leading to the full delivery of capacity of active materials at low discharge current. On the other hand, the coating carbon is inactive, higher carbon content may lead to the decrease of discharge capacity. But the electronic conductivity and particle size of materials show a more obvious effect on the high-rate dischargeability. The initial discharge capacities of $LiFePO_4$ samples at 5*C* rate are 85.0, 105.5, 116.0 and 114.2 mAh g^{-1}, respectively, suggesting that sample LFP3 has the best high-rate dischargeability. The better dischargeability of sample LFP3 could be attributed to its uniform carbon coating, which leads to the decrease of particle size and the increase of electronic conductivity. Although sample LFP4 also has the complete carbon coating, the excessive carbon cannot help to restrict the particle growth. On the contrary, the excessive inactive carbon coating could impedes charge-transfer through the cathode, thus leading to the decrease of discharge capacity at high rates. The materials with high carbon content also exhibit excellent cycling performance. As shown in Fig. 9, the discharge capacity of sample LFP3 could reach 135 mAh g^{-1} after 100 cycles at 2*C* rate, near to its initial capacity of 138 mAh g^{-1}.

4. Conclusions

The effects of synthesis temperature and carbon content on the performance of $LiFePO_4$/C composites are investigated systematically in this paper. The results show that the carbonization degree and the content of sp^2-type graphitized structure in conductive carbon increase with the synthesis temperature increasing, thus leading to the improvement of electronic conductivity and electrochemical performance of materials. The carbon content determines the quality of carbon coating on the $LiFePO_4$ particle surface, and only a proper carbon content (about 3%) could lead to a more complete and uniform carbon distribution and, consequently, a more homogeneous and small particle size of $LiFePO_4$/C composite materials. The optimal sample synthesized at 700 °C and with a carbon content of 3.1%, exhibits excellent high-rate dischargeability and cycling performance, whose discharge capacity could reach 116.0 mAh g^{-1} at 5*C* rate, and the discharge capacity shows little degradation after 100 cycles at 2*C* rate.

References

[1] A.K. Padhi, K.S. Nanjundaswamy, J.B. Goodenough, J. Electrochem. Soc. 144 (1997) 1188.
[2] G. Song, Y. Wu, G. Liu, Q. Xu, J. Alloys Compd. 487 (2009) 214–217.
[3] A.Y. Shenouda, H.K. Liu, J. Alloys Compd. 477 (2009) 498–503.
[4] A.A. Salah, A. Mauger, C.M. Julien, F. Gendron, Mater. Sci. Eng. B 129 (2006) 232–244.
[5] Y. Wang, Y. Yang, X. Hu, Y. Yang, H. Shao, J. Alloys Compd. 481 (2009) 590–594.
[6] V. Drozd, G.Q. Liu, R.S. Liu, H.T. Kuo, C.H. Shen, D.S. Shy, X.K. Xing, J. Alloys Compd. 487 (2009) 58–63.
[7] H. Chen, S.Z. Wang, Mater. Lett. 63 (2009) 1668.
[8] Y. Wang, Y. Wang, E. Hosono, K. Wang, H. Zhou, Angew. Chem. Int. Ed. 47 (2008) 7461–7465.
[9] T. Hirose, T. Fujino, T. Fan, H. Endo, T. Okabe, M. Yoshimura, Carbon 40 (2002) 761–765.
[10] R. Kostecki, B. Schnyder, D. Alliata, X. Song, K. Kinoshita, Thin Solid Films 396 (2001) 36–43.
[11] Z. Chen, J.R. Dahn, J. Electrochem. Soc. 149 (2002) A1184–A1189.
[12] M.M. Doeff, J.D. Wilcox, R. Kostecki, G. Lau, J. Power Sources 163 (2006) 180–184.
[13] T. Nakamura, Y. Miwa, M. Tabuchi, Y. Yamada, J. Electrochem. Soc. 153 (2006) A1108–A1114.
[14] Y. Isono, A. Yoshida, Y. Hishiyama, Y. Kaburagi, Carbon 42 (2004) 1799–1805.
[15] Y. Hu, M.M. Doeff, R. Kostecki, R. Finones, J. Electrochem. Soc. 151 (2004) A1279.
[16] F. Gao, Z. Tang, Electrochim. Acta 53 (2008) 5071–5075.
[17] H.C. Shin, W.I. Cho, H. Jang, J. Power Sources 159 (2006) 1383–1388.
[18] H.H. Chang, C.C. Chang, C.Y. Su, H.C. Wu, M.H. Yang, N.L. Wu, J. Power Sources 185 (2008) 466–472.